



# Intelligent road adaptive suspension system design using an experts' based hybrid genetic algorithm



Stratis Kanarachos<sup>a,\*</sup>, Andreas Kanarachos<sup>b</sup>

<sup>a</sup> Faculty of Engineering & Computing, Coventry University, Coventry CV12JH, UK

<sup>b</sup> Mechanical Engineering Department, Frederick University, Nicosia 1093, Cyprus

## ARTICLE INFO

### Article history:

Available online 2 July 2015

### Keywords:

Intelligent suspension system  
Road adaptive  
Hybrid genetic algorithms

## ABSTRACT

There is an increasing demand for vehicles suitable for both on and off road driving characterized by superior comfort and handling performance. This is problematic for most suspension systems because there is a trade off balance between vibration reduction, suspension travel, actuator effort, road holding capability, as well as noise and fatigue requirements. Only in the UK every 11 min a car is getting damaged because of potholes. In this paper, a method to design an intelligent suspension system with the objective to overcome the trade-off barrier using the smallest actuator is presented. An experts' based algorithm continuously monitors the road excitation in relation to the suspension travel and adapts accordingly the suspension system. It is shown that by applying genetic algorithm it is possible to optimally tune the system. However, the global optimum is hard to find due to the problem nonlinearity. A hybrid genetic algorithm that improves the probability of successfully finding the best design is presented. The simulation results show that the proposed intelligent system performs for – well known in the literature scenarios – better than others and remarkably this is achieved by reducing the actuator's size.

© 2015 Elsevier Ltd. All rights reserved.

## 1. Introduction

There is an increasing demand for vehicles suitable for both on and off road driving characterized by superior performance. Only in the UK every 11 min a car is getting damaged because of potholes. The major design targets of a vehicle suspension system are to isolate the driver and vehicle from road irregularities such as a bumps, pot holes, unpaved surfaces and to maximize its road holding performance (Song, Zhao, Wang, & Niu, 2014). It is well known that a linear passive suspension system cannot satisfy all requirements simultaneously. A passive soft suspension will reduce acceleration and maximum road induced forces at the cost of increased wheel hopping, which eventually reduces road grip. The opposite happens with a hard suspension. Many solutions such as active and semi-active suspension have been proposed in the past (Gohrle, Schindler, Wagner, & Sawodny, 2014). In view of the complexity and power demands for active suspension systems the design interest nowadays is focusing on semi-active suspensions. These seem to cope with the latest demands for car production, customer interests and needs and also with the latest developments in the area of electronics, sensors, tunable dampers

and magneto- and electro-rheological actuators (Poussot-Vassal, Spelta, Sename, Savaresi, & Dugard, 2012).

Previous research focused more on suspension feedback control and has been investigated extensively in the last decade for active and semi-active suspension concepts. There exist various control concepts like the linear-quadratic (LQ) state-vector feedback, neural networks, clipped control,  $H_\infty$  controllers, fuzzy control, etc (Brezas, Smith, & Hault, 2015; Kanarachos, 2012; Soleymani, Montazeri-Gh, & Amiryan, 2012; Tung, Juang, Lee, Shieh, & Wu, 2011; Tusset, Rafikov, & Balthazar, 2009). In conclusion, all control concepts aim at introducing additional forces to the suspension system, while the physical structure of actuators and sensors determines the final control system design.

Designing a suspension system is generally a hard task because the problem is multi-objective and highly nonlinear due to system's nonlinearities like limits of the rattle space distance, of the actuators dynamics (power and force limits), the nonlinearities embedded in the control law and also fatigue requirements (amplitude and number of cycles). A powerful tool for solving such problems is experts' knowledge and global optimization (Kanarachos, Koulocheris, & Spentzas, 2005). For example, in passive suspension system design particle swarm optimization and genetic algorithm were innovatively combined for Pareto optimal design of a five-degree of freedom vehicle vibration model (Mahmoodabadi, Adljooy Safaie, Bagheri, & Nariman-Zadeh, 2013). Poussot-Vassal et al. (2008)

\* Corresponding author. Tel./fax: +44 (0)2477657720.

E-mail addresses: [stratis.kanarachos@coventry.ac.uk](mailto:stratis.kanarachos@coventry.ac.uk) (S. Kanarachos), [eng.ka@frederick.ac.cy](mailto:eng.ka@frederick.ac.cy) (A. Kanarachos).

**Nomenclature**

$m_1$	sprung mass
$m_2$	unsprung mass
$c_1$	damping constant
$D$	artificial damping constant
$k_1$	spring constant
$k_2$	tire vertical stiffness
$z_0$	road disturbance
$z_1$	sprung mass displacement
$z_2$	un-sprung mass displacement
$\bar{z}_R$	estimated rattle space distance
$z_0(t)$	road disturbance
$z_{0d}(t)$	deterministic road disturbance
$z_{0r}(t)$	stochastic road disturbance
$z_{Rlim}$	rattle space distance limit
$z_{flim}$	tire deflection limit
$f_{act}$	actuator force
$f_{clim}$	actuator force limit

$f_c$	control force
$T_{act}$	actuator force time constant
$T_{pred}$	control law constant
$z_{switch}$	control law constant
$f_{actlim}$	control law constant
$\dot{u}$	control input rate
$u$	control input
$v$	parameter set

**Subscripts**

$i$	iteration
$opt$	optimized
$\mu$	mean value
$\sigma$	standard deviation

**Superscript**

$j$	population member
-----	-------------------

formulated the semi-active suspension design as a Linear Parameter Varying Problem and solved the resulting Linear Matrix Inequalities problem using genetic algorithm. In active suspension evolutionary algorithms, such as the cultural and niche algorithm, were combined to design a Fuzzy-PID controller and optimize control rules (Wang et al., 2015).

Although standard control design methods add valuable knowledge to the design of a vehicle suspension system, the problem itself is a system design problem with non-negligible nonlinearities, which – and this is interesting – can positively contribute to the optimization of the design. A step in this direction was taken in (Huang, Lin, & Chen, 2010) in which a road adaptive suspension system is presented. That line of thought is extended in this paper by designing an intelligent road adaptive suspension system. An experts' based algorithm continuously monitors the road input in relation to the suspension travel and determines the system behavior. The main objective is to optimize system performance, overcome the trade-off barrier and minimize the size of the actuator. A large actuator has increased space requirements, is noisier, consumes more energy and induces higher loads to the vehicle structure. The overall system performance is optimized using genetic algorithm. It is shown that the direct application of genetic algorithm does not always lead to the optimum solution. In this context, an automated design procedure that improves the probability of success has been developed and is described. The simulation results show that the proposed intelligent system performs better for – well known in the literature scenarios – than others and remarkably this is achieved by reducing the actuator's size.

The rest of the paper is organized as follows: In Section 2 the mathematical model of the vehicle is presented. In Section 3 the intelligent suspension system is explained. The numerical results are illustrated and discussed in Section 4. In Section 5 details and practical guidelines on how to apply the genetic algorithm are given. In Section 6 conclusions and future research directions are drawn.

**2. The system model****2.1. The quarter-car model**

When suspension modeling and control are considered, the well-known vertical quarter-car model is often used (Brown, Pusey, Murugan, & Le, 2013; Koch, Fritsch, & Lohmann, 2010).

This model allows studying the vertical behavior of a vehicle according to the suspension type (Savaresi, Poussot-Vassal, Spelta, Sename, & Dugard, 2010). More advanced models can be used for studying the pitch and roll motion of the vehicle but the vertical behavior, comfort and chassis forces in this direction can be mainly determined using this simple model.

The mathematical model with semi-active suspension is shown in Fig. 1. Wheel and axle (unsprung mass  $m_2$ ) are connected to the car body through a passive spring with the spring coefficient  $k_1$ , a modulated damper with the passive damping coefficient  $c_1$  and a variable force element  $f_{act}(t)$ , while the tire is modeled as a spring  $k_2$ . The car body is represented by the mass  $m_1$  and the road disturbance by  $z_0(t)$ . The equations of motion of the vehicle are the following:

$$\begin{aligned} m_1 \ddot{z}_1 + c_1(\dot{z}_1 - \dot{z}_2) + k_1(z_1 - z_2) - f_{act} &= 0 \\ m_2 \ddot{z}_2 - c_1(\dot{z}_1 - \dot{z}_2) - k_1(z_1 - z_2) + f_{act} + k_2(z_2 - z_0) &= 0 \end{aligned} \quad (1)$$

where  $z_1$  is the displacement of the sprung mass and  $z_2$  is the displacement of the unsprung mass.

**2.2. Road disturbances**

Of major importance for the lay out of the suspension is the definition of the road disturbances. The road disturbances must mirror the real driving conditions and include discrete disturbances  $z_{0d}(t)$

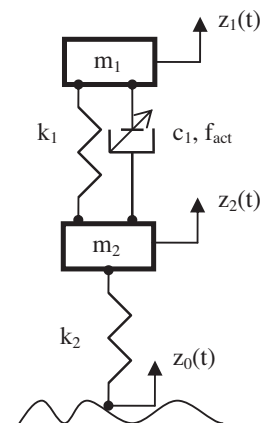


Fig. 1. Quarter car model with semi-active suspension.

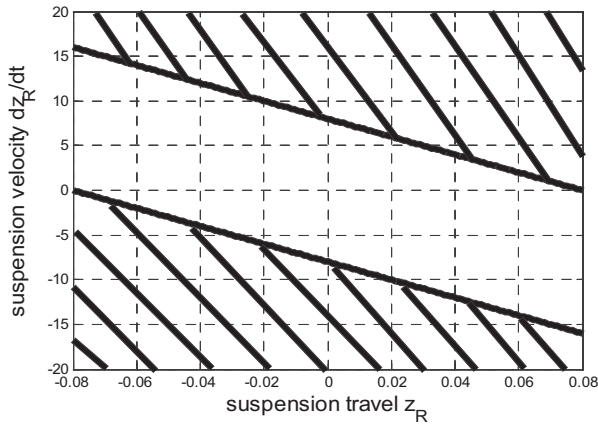


Fig. 2. Operating envelope of passive (clear) and active (hatch) suspension system for  $\bar{z}_R = 0.08$  m and  $T_{pred} = 0.01$  s.

(e.g. bump, pot hole, cobbled road) and stochastic ones  $z_{or}(t)$  (e.g. off-road driving). Suspension design considering only one road disturbance scenario (e.g. a bump) is not robust enough and may lead to unsatisfactory performance in other cases. In this study, two typical road disturbances have been selected and are described in Eq. (2).

$$z_{od}(t) \begin{cases} = A_b \cdot (1 - \cos(8\pi t))/2 & \text{for } 0 \leq t \leq 0.25 \text{ sec; } (A_b = 11 \text{ cm}) \\ = 0 & \text{for } t > 0.25 \text{ sec} \end{cases}$$

$$z_{or}(t) = \text{random road profile} \tag{2}$$

where  $A_b$  is the bump's maximum road height value and  $z_{or}(t)$  a filtered white noise signal (Kanarachos, 2012).

2.3. Actuator model

In many design studies the performance limits of the actuator are neglected. Nevertheless, their influence can be significant (Isermann, 2003). For the purpose of this case study we include the dynamic performance of the actuator, which is described by a first order transfer function (Nguyen & Choi, 2009):

$$\dot{f}_{act} \cdot T_{act} + f_{act} = f_c \tag{3}$$

with the time constant  $T_{act}$ , describing the so called control input rate  $\dot{u}$  limit of the actuator.

Like any mechanical device, the force generated by the actuator is limited. The maximum actuator force is included in the actuator model, which is denoted as  $f_{actlim}$ :

$$|f_{act}| \leq f_{actlim} \tag{4}$$

2.4. System constraints

The system has to fulfil constraints that are dependent on space requirements and tire dimensions. First, the relative displacement

between the sprung and un-sprung mass  $z_R$  is restricted by the design constraint:

$$|z_1 - z_2| \leq z_{Rlim} \tag{5}$$

with  $z_{Rlim}$  denoting the maximum allowed rattle space distance. The absolute value denotes that this restriction is independent of the direction of the road disturbance (bump or pot hole). Second, the tire deflection should be limited in order to guarantee a certain road holding performance:

$$|z_2 - z_r| \leq z_{rlim} \tag{6}$$

where  $z_{rlim}$  is the prescribed tire deflection limit.

3. The intelligent road adaptive suspension system

In order to incorporate the above constraints in a solution procedure it is necessary to recall Pontryagin's maximum principle. Pontryagin's principle refers to the best possible input for taking a dynamical system from one state to another, especially in the presence of constraints for the state and/or inputs (Naidu, 2002). The principle states that the Hamiltonian must be minimized over the set of all permissible inputs. Applying the principle to minimum time problems with constrained input the optimum result is, as well known, a switched bang-bang (-1/+1) input. The advantage of Pontryagin's principle is that it holds even for nonlinear systems contrary to other linear theories. However, the solution of the adjoint equations using the Hamiltonian function has a large computational cost and it is not possible to use it in real time applications. Thus, the target consists in reality in the elaboration of an expert solution that can resemble Pontryagin's principle.

For creating a general solution the outcome of Pontryagin's principle is utilized. It is assumed that the optimized solution has a bang-bang form the amplitude of which is unknown. The target is to optimize the system performance for the smallest amplitude. Furthermore, in order to reduce the actuator's effort the system operates between two modes: a passive and an active one. For normal road conditions the system operates in passive mode and only when necessary switches to the other one. When to switch, how to switch and how the structure of the active part looks like is described by a rule based algorithm that has been derived based on experts' knowledge. The algorithm is comprised out of three levels.

The first level focuses on monitoring the road disturbance in relation to the suspension travel. It assumes that both the rattle space distance  $z_R$  and velocity  $\dot{z}_R$

$$z_R = z_1 - z_2, \quad \dot{z}_R = \dot{z}_1 - \dot{z}_2 \tag{7}$$

can be measured or estimated (Yim, Seok, & Lee, 2012). The projected rattle space distance  $\bar{z}_R$  for a prescribed or given prediction time  $T_{pred}$  can then be computed from a first order Taylor approximation:

$$\bar{z}_R = (z_1 - z_2) + T_{pred}(\dot{z}_1 - \dot{z}_2) \tag{8}$$

This information serves for the activation of the modulated part of the damper in the following sense:

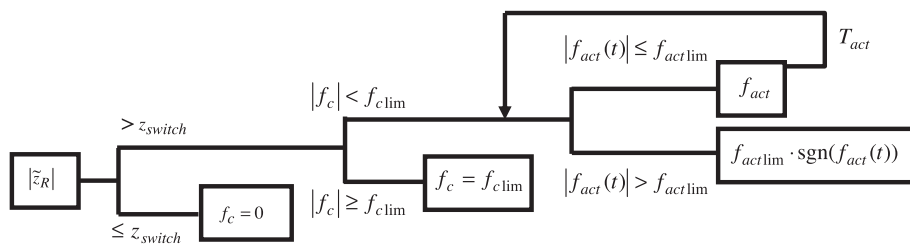


Fig. 3. Operating envelope of passive (clear) and active (thick dashed) suspension element for  $\bar{z}_R = 0.08$  m and  $T_{pred} = 0.01$  s.

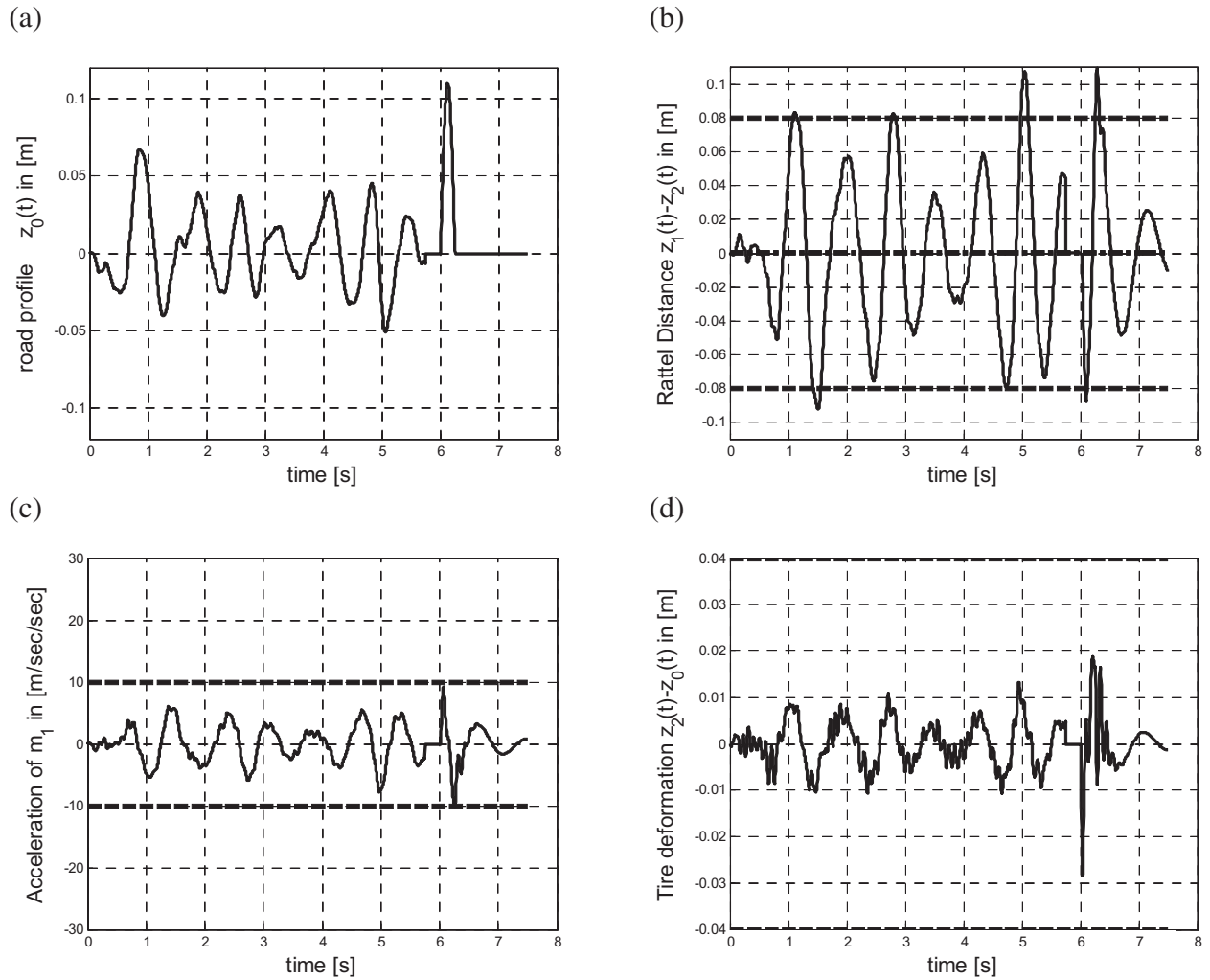


Fig. 4. Numerical results for passive suspension system: (a) road profile  $z_0$ ; (b) rattle space displacement  $z_2-z_1$ ; (c) sprung mass acceleration  $\dot{z}_1$ ; and (d) tire deformation  $z_2-z_0$ .

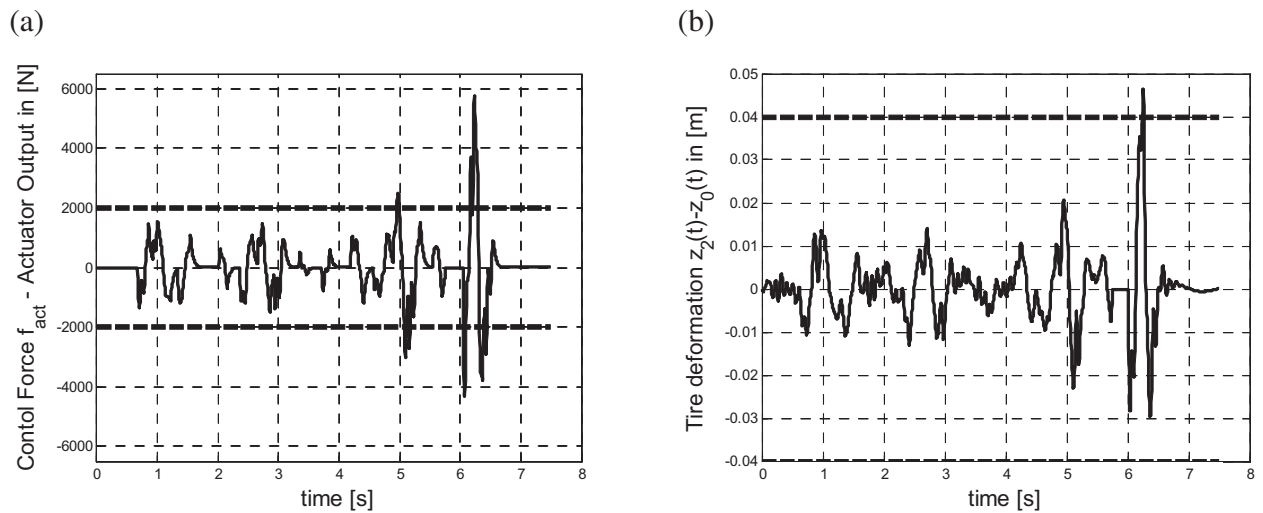
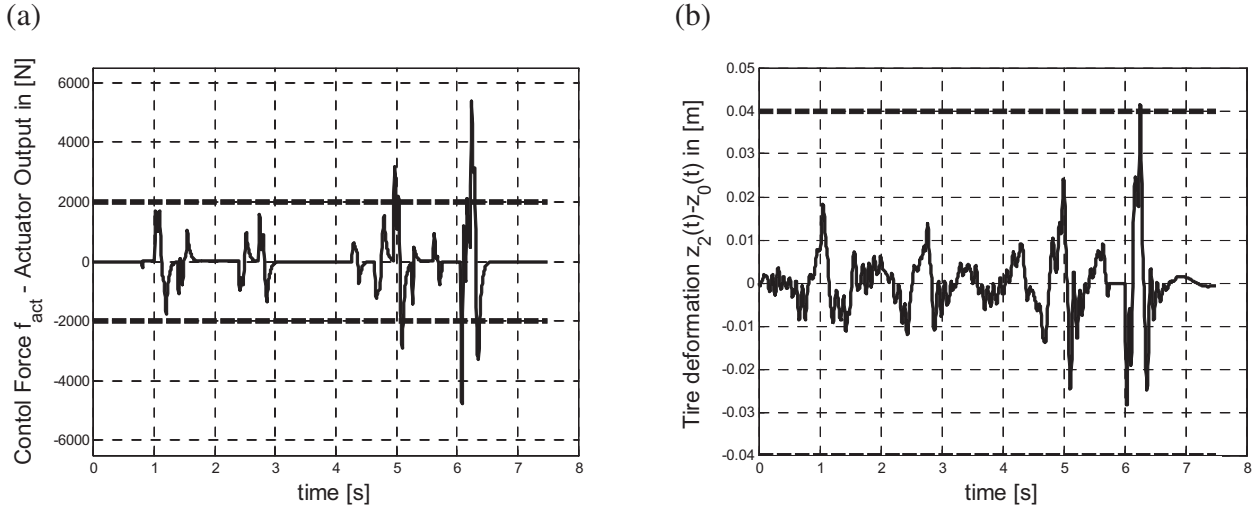


Fig. 5. Numerical results for the intelligent system with  $z_{switch} = 0.02$  m ( $D = 7$ ,  $T_{act} = 0.04$  s,  $T_{pred} = 0$ , linear control,  $f_{actlim} = \infty$ ,  $f_{clim} = \infty$ ): (a) actuator force  $f_{act}$ ; (b) tire deformation  $z_2-z_0$ .



**Fig. 6.** Numerical results for the intelligent system with  $z_{switch} = 0.05$  m ( $D = 10.4$ ,  $T_{act} = 0.04$  s,  $T_{pred} = 0$ , linear control,  $f_{actlim} = \infty$ ,  $f_{clim} = \infty$ ): (a) actuator force  $f_{act}$ ; (b) tire deformation  $z_2 - z_0$ .

$$f_c = \begin{cases} \neq 0 & \text{if } |\dot{z}_R| > z_{switch} \\ otherwise = 0 & \end{cases} \quad (9)$$

with  $z_{switch}$  being a prescribed constant. By introducing the “prediction element”  $\dot{z}_R$  the system becomes more intelligent because it varies the structure not only depending on how close to the travel limit the system operates but also on the rate at which it approaches it. A graphical illustration of the concept is shown in Fig. 2. In case the predicted rattle space distance violates the limits an additional control force is generated. Hence, the active part is utilized only when needed.

In the second part the current formulation limits the maximum actuator force by design, according to Pontryagin’s principle:

$$f_c = f_c(z_1, z_2, \dot{z}_1, \dot{z}_2) = \begin{cases} -D \cdot (\dot{z}_1 - \dot{z}_2), & |f_c| \leq f_{clim} \\ f_{clim}, & |f_c| > f_{clim} \end{cases} \quad (10)$$

where  $D$  is an artificial damping constant and  $f_{clim}$  is the “saturation element”. The value of the saturation element is part of the optimization problem. In general, it is desirable to achieve the best performance for a low  $f_{clim}$  limit. If this is the case then it is expected

**Table 1**

Performance of the intelligent suspension for  $z_{switch} = 0-0.05$  m ( $T_{act} = 0.04$  s,  $T_{pred} = 0$ ,  $f_{actlim} = \infty$ ,  $f_{clim} = \infty$ ).

	$z_{switch}$ [m]				
	0	0.02	0.03	0.04	0.05
Max $ f_{act} $ [N]	6347	5690	5670	5562	5390
Max $ z_R $ [m]	0.08	0.08	0.08	0.08	0.08
Max $ \dot{z}_1 $ [m/s <sup>2</sup> ]	28.4475	26.1609	25.997	25.358	24.18

that the actuator force will quickly saturate and thus resemble the output of Pontryagin’s principle.

The third part of the controller refers to filtering the input signal and smoothing out the transition between passive and active mode. The control force command is filtered using a nonlinear first order function, as follows:

$$\dot{f}_{act} \cdot T_{act} + f_{act} = f_c \quad f_{act}(t) \begin{cases} = f_{act}(t), & |f_{act}(t)| \leq f_{actlim} \\ = f_{actlim} \cdot \text{sgn}(f_{act}(t)), & |f_{act}(t)| > f_{actlim} \end{cases} \quad (11)$$

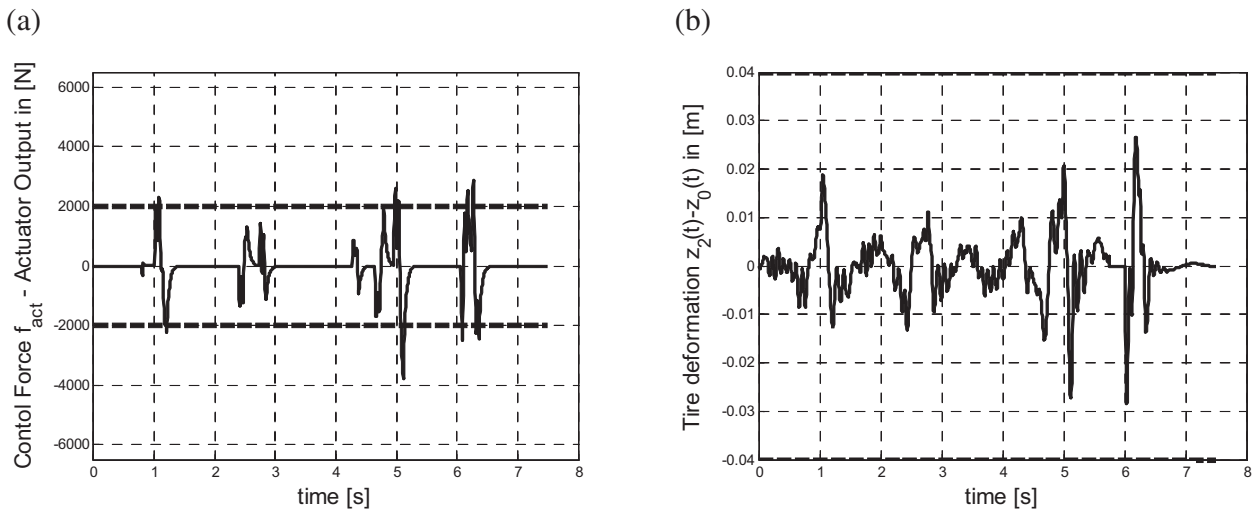


**Fig. 7.** Numerical results for the intelligent system with  $f_{clim} = 5000$  N and  $z_{switch} = 0.05$  m. ( $D = 17.73$ ,  $T_{act} = 0.04$  s,  $T_{pred} = 0$ , linear control,  $f_{actlim} = \infty$ ): (a) actuator force  $f_{act}$ ; (b) tire deformation  $z_2 - z_0$ .

**Table 2**

Performance of the intelligent suspension for  $f_{clim} = 5000$  N. ( $z_{switch} = 0.02 \dots 0.05$  m,  $T_{act} = 0.04$  s,  $T_{pred} = 0$ , linear control,  $f_{actlim} = \infty$ ).

	$z_{switch}$ [m]			
	0.02	0.03	0.04	0.05
Max $ f_{act} $ [N]	4263	3829	3181	2807
Max $ z_R $ [m]	0.0726	0.0735	0.0776	0.0794
Max $ \ddot{z}_1 $ [m/s <sup>2</sup> ]	18.641	17.4677	15.7996	14.7899

**Table 3**

Performance of the intelligent system for  $f_{clim} = 4000$  N, ( $z_{switch} = 0.02 \dots 0.05$  m,  $T_{act} = 0.04$  s,  $T_{pred} = 0$ , linear control,  $f_{actlim} = \infty$ ).

	$z_{switch}$ [m]		
	0.02	0.03	0.04
Max $ f_{act} $ [N]	3694	3425	2743
Max $ z_R $ [m]	0.0733	0.0756	0.0784
Max $ \ddot{z}_1 $ [m/s <sup>2</sup> ]	16.3408	15.4339	14.1141

where  $T_{act}$  is a constant representative of actuators' dynamics and  $f_{actlim}$  is a control law constant.

A schematic of the experts' based algorithm is shown in Fig. 3.

**4. Numerical results – analysis of the design parameters**

The proposed intelligent suspension system is influenced by a number of parameters that have to be tuned optimally. In this context, the performance of the passive suspension system (basis) is first presented and then the influence of the design parameters is progressively studied and discussed.

**4.1. Passive vibration suspension system and optimization target**

A passive suspension system with the following parameters is considered:

$$\begin{aligned}
 m_1 &= 289 \text{ kg} & m_2 &= 59 \text{ kg} \\
 c_1 &= 1000 \text{ N/(m/s)} \\
 k_1 &= 190000 \text{ N/m} & k_2 &= 16912 \text{ N/m} \\
 z_{Rlim} &= 8 \text{ cm} & z_{tlim} &= 4 \text{ cm}
 \end{aligned}
 \tag{12}$$

In Fig. 4(a) the assumed road excitation consisting of a random (off-road) part during the first 5.75 s and a deterministic one (a bump with the amplitude of 11 cm) beginning at 6 s is shown.

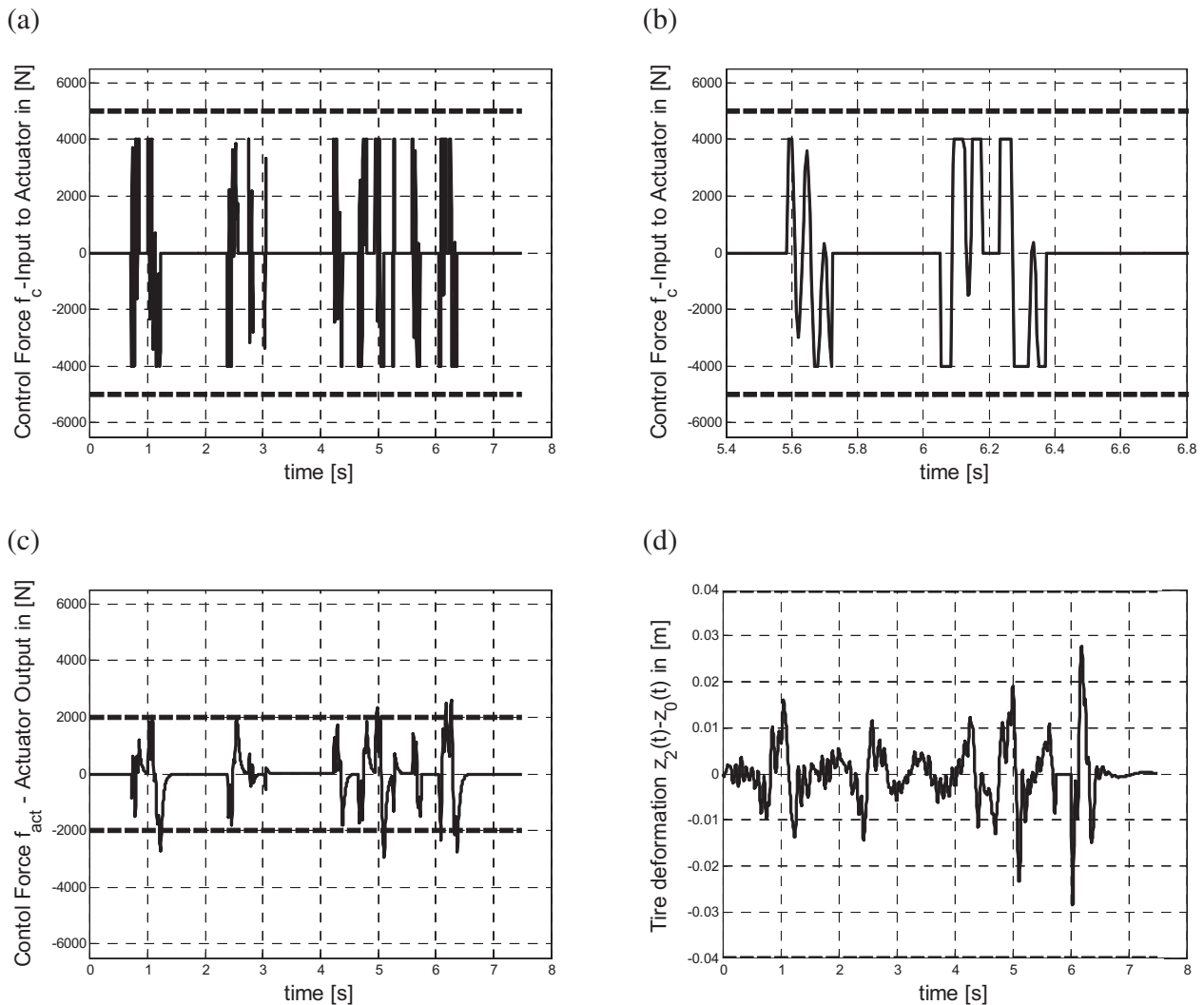


**Fig. 8.** Numerical results for the intelligent system with  $f_{clim} = 4000$  N and  $z_{switch} = 0.04$  m ( $D = 21.1$ ,  $T_{act} = 0.04$  s,  $T_{pred} = 0$ ,  $f_{actlim} = \infty$ ): (a) control input  $f_c$ ; (b) control input  $f_c$  for  $5.4 \leq t \leq 6.8$  s; (c) actuator force  $f_{act}$ ; (d) tire deformation  $z_2 - z_0$ .



**Table 4**

Performance of the intelligent system for  $f_{actlim} = 2000$  N, ( $z_{switch} = 0.02\text{--}0.05$  m,  $T_{act} = 0.04$  s,  $T_{pred} = 0$ ,  $f_{clim} = \infty$ ).

	$z_{switch}$ [m]		
	0.02	0.03	0.04
Max $ f_{act} $ [N]	2000	2000	2000
Max $ z_R $ [m]	0.0766	0.077	0.0789
Max $ \ddot{z}_1 $ [ $m/s^2$ ]	13.2535	13.4830	13.6634

The combination of a stochastic road profile with a deterministic profile is very important and avoids training a system for a specific case only. In Fig. 4(b)–(d) the response of the system is shown.

The corresponding rattle distance  $z_1 - z_2$  is shown in Fig. 4(b). The dashed lines point out the rattle space limit  $z_{Rlim}$ . The condition  $|z_R| \leq z_{Rlim}$  is violated for both road (random and bump) disturbances. The maximum value for the rattle space distance is  $\max z_R = 0.1098$  m  $> z_{Rlim}$  and the maximum absolute acceleration equal to  $\max |\ddot{z}_1| = 10.0012$   $m/s^2$  (see Fig. 4(b) and (c) respectively). In Fig. 4(c) the dashed lines indicate the maximum acceleration  $\max |\ddot{z}_1|$ . This value serves as a basis for the rest of the analysis. In Fig. 4(d) the tire deformation  $z_t = z_2 - z_r$  is shown and the dashed lines indicate the tire deformation limit  $z_{tlim}$ . In following figures the rattle space limit  $z_{Rlim}$ , tire deformation limit  $z_{tlim}$  and maximum acceleration  $\max |\ddot{z}_1| = 10.0012$   $m/s^2$  are illustrated for comparison reasons.

The optimization target for the layout of the intelligent suspension system is the minimization  $\ddot{z}_1$  of the car body's acceleration  $m_1$ :

$$|\ddot{z}_1| = \text{Minimum} \quad (13)$$

using the smallest actuator  $\min(\max(f_{actlim}))$  while fulfilling the various system constraints, see Eqs. 4–6. The main parameters for the synthesis are:

sprung mass :  $m_1$

Actuator :  $T_{act}, f_{actlim}$  (14)

Controller :  $T_{pred}, z_{switch}, f_{clim}, D$

In the following the assumption is made that the sprung mass  $m_1$  is known (see Eq. (12)). In case the carriage mass varies considerably, additional investigations become necessary to answer if  $m_1$  must – in any case – be estimated or measured or even if a more

**Table 5**

Performance of the intelligent system for  $f_{actlim} = 1500$  N ( $z_{switch} = 0.02\text{--}0.05$  m,  $T_{act} = 0.04$  s,  $T_{pred} = 0$ ,  $f_{clim} = \infty$ ).

	$z_{switch}$ [m]		
	0.02	0.03	0.04
Max $ f_{act} $ [N]	1500	1500	1500
Max $ z_R $ [m]	0.078	0.0796	0.08
Max $ \ddot{z}_1 $ [ $m/s^2$ ]	11.6971	12.0039	13.0288

robust suspension can be effectively designed. However, even in this case where  $m_1$  is known, the optimization problem (13) is complex enough due to the presence of the rattle distance (state variables) and the actuator (control variables) constraints.

For the cases presented, in the remaining part of this section, the design parameters  $T_{act}, f_{actlim}, T_{pred}, z_{switch}, f_{clim}$  have known values and only parameter  $D$  is unknown. The optimisation problem, see Eqs. (13) and (14), is solved by genetic algorithm and in particular using the ga function in Matlab. The starting value for the optimisation is  $D = 0$ , which gives the best results according to the authors. Details regarding the implementation of the genetic algorithm are given in Section 5.

#### 4.2. Investigation of the properties of the switching function

For investigating the properties of the switching function it is assumed that  $f_{actlim} = \infty, f_{clim} = \infty$ , the actuator time constant is  $T_{act} = 0.04$  s and the prediction time is  $T_{pred} = 0$ . In this case the optimisation problem, Eq. (13), concerns only parameter  $D$ .

If  $z_{switch}$  is varied between  $z_{switch} = 0$  (no switching, the suspension is active all the time) and  $z_{switch} = 0.05$  m the following results are obtained:

The high accelerations  $|\ddot{z}_1|$  come out mainly when limiting the suspension travel caused by the bump. Two characteristic cases are displayed in Figs. 5 and 6. In case of an “early” switch limit ( $z_{switch} = 0.02$  m) the maximum attained acceleration is  $\max |\ddot{z}_1| = 26.16$   $m/s^2$  and the maximum actuator force  $\max |f_{act}| = 5690$  N, while for a “late” switch limit ( $z_{switch} = 0.05$  m) the maximum attained acceleration is  $\max |\ddot{z}_1| = 24.18$   $m/s^2$  and the maximum actuator force  $\max |f_{act}| = 5390$  N. With a smaller actuator force  $\max$  a lower acceleration level  $\max$  is achieved. In both cases the tire deformation limit is exceeded. The analysis shows that a more sophisticated system is necessary for reducing the

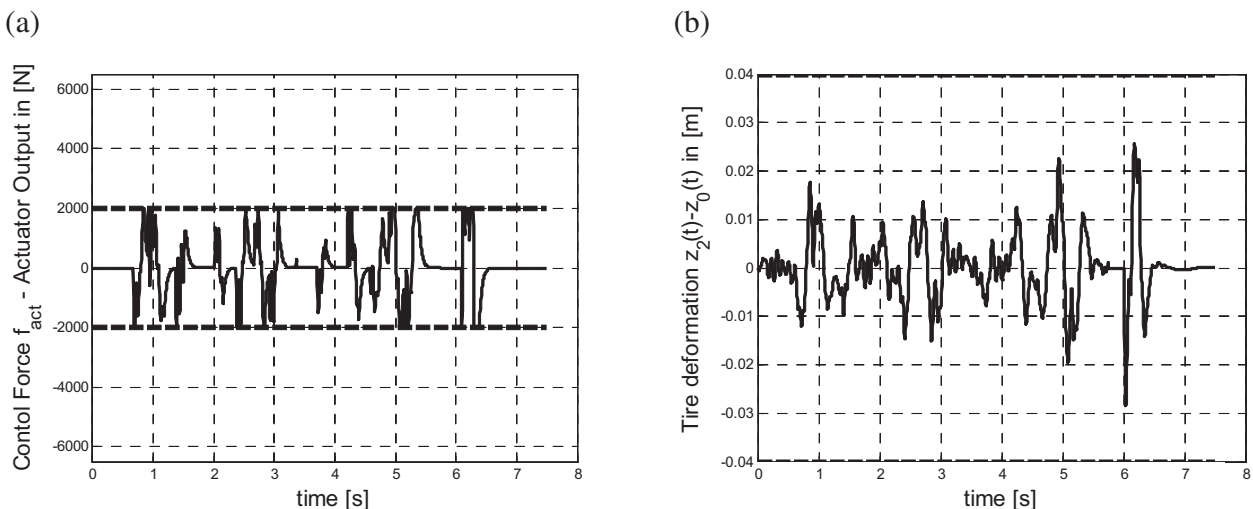


**Fig. 9.** Numerical results for the intelligent system with  $f_{actlim} = 2000$  N and  $z_{switch} = 0.03$  m, ( $D = 17.7$ ,  $T_{act} = 0.04$  s,  $T_{pred} = 0$ ,  $f_{clim} = \infty$ ): (a) actuator force  $f_{act}$ ; (b) tire deformation  $z_2 - z_0$ .

acceleration of the vehicle carriage without degrading its road holding performance.

4.3. Investigation of the saturation limit's properties

The system is designed to include a saturation limit for the active part, as defined in Eq. (4). A simple limiter that constrains the control input  $f_c$  characterizes the actuator's output according to the following equation:

$$f_c(t) \begin{cases} = f_c(t) & \text{if } |f_c(t)| \leq f_{c\text{lim}} \\ = f_{c\text{lim}} \cdot \text{sgn}(f_c(t)) & \end{cases} \quad (15)$$

For exploring the influence of the above nonlinear filter the parameter is set to the value of  $f_{c\text{lim}} = 5000$  N and  $f_{c\text{lim}} = 4000$  N, while  $z_{\text{switch}}$  is again varied between 0.02 and 0.04 m. The results for  $f_{c\text{lim}} = 5000$  N are shown in Table 2 and Fig. 7, while the results for  $f_{c\text{lim}} = 4000$  N are shown in Table 3 and Fig. 8.

As observed from, Fig. 8(a) and (b), the suspension system succeeds in creating a bang-bang control input that resembles Pontryagin's principle. The vehicle carriage acceleration is reduced from 24.180 m/s<sup>2</sup> (see Table 1) to 14.1141 m/s<sup>2</sup> (see Table 3). This is a considerable reduction for the problem under consideration.

4.4. Investigation of the properties of the nonlinear smoothing filter

In order to further reduce the acceleration the system is designed taking into consideration the actuator dynamics. The constraint of the actuator dynamics is a natural constraint due to the limit of the actuator power and is independent of the used mathematical model (1st, 2nd or higher order linear or nonlinear transfer function) of the actuator.

In the present case the actuator is modeled as a 1st order transfer function with a constrained output according to Eq. (11). This constraint is set to the values of  $f_{\text{actlim}} = 2000$  N and  $f_{\text{actlim}} = 1500$  N while  $z_{\text{switch}}$  is again varied between 0.02–0.04 m. The results for  $f_{\text{actlim}} = 2000$  N are shown in Table 4 and Fig. 9, while the results for  $f_{\text{actlim}} = 1500$  N are shown in Table 5 and Fig. 10.

The results show that the nonlinear smoothing filter succeeds in creating a partially bang-bang output signal which reduces the vehicle carriage acceleration from 24.180 m/s<sup>2</sup> (see Table 1) to 11.6971 m/s<sup>2</sup> (see Table 5). This is a 52% reduction of the maximum acceleration while the maximum tire dynamic load has remained exactly in the same range.

It is noted that the performance improvement is achieved with a significantly smaller actuator. The maximum acceleration  $\ddot{z}_1$  is 11.6971 m/s<sup>2</sup> and achieved with  $f_{\text{act}} = 1500$  N (Table 5), while with  $f_{\text{act}} = 3694$  N (Table 3) it is 16.3408 m/s<sup>2</sup>. Thus, the maximum

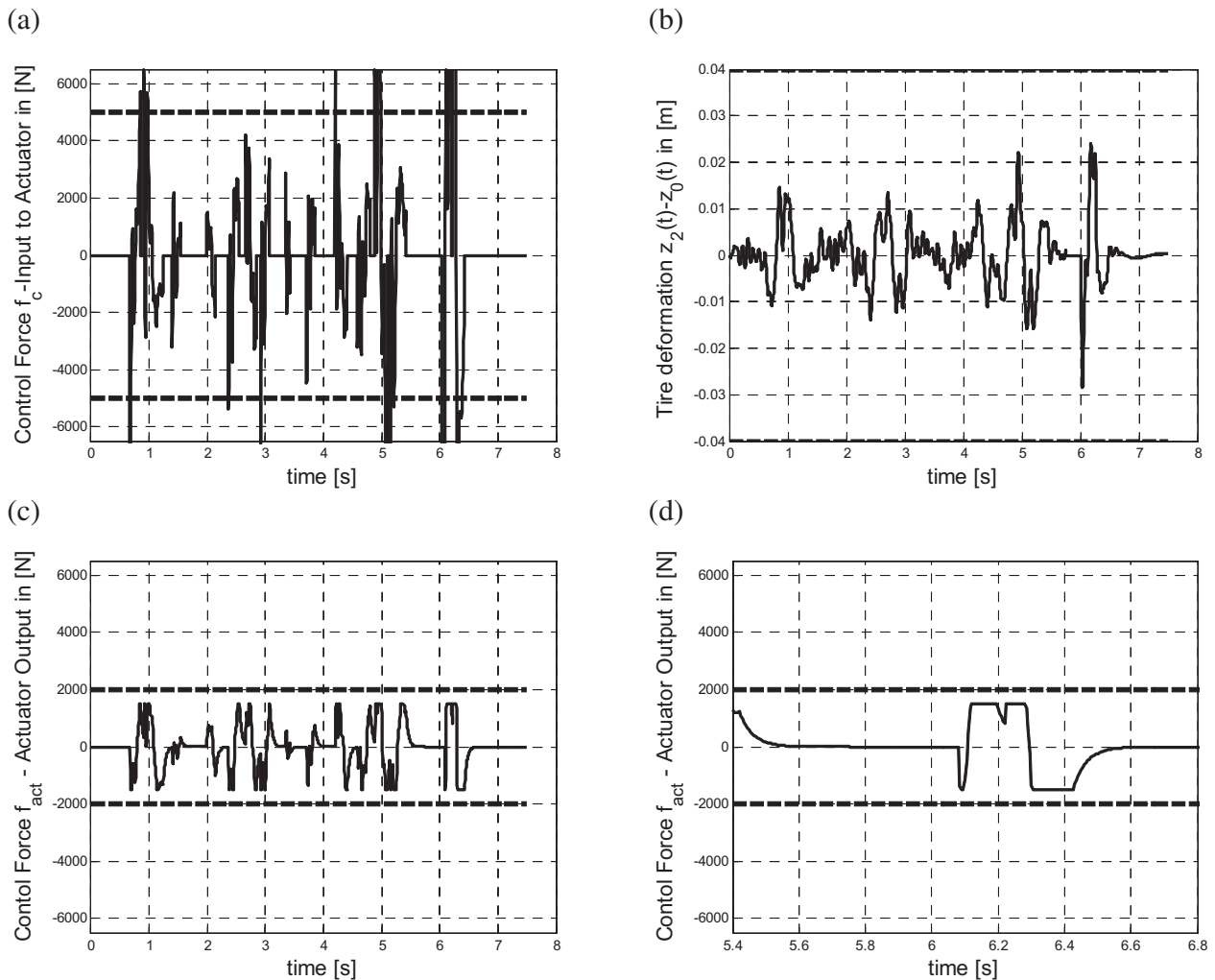


Fig. 10. Numerical results for the intelligent system with  $f_{\text{actlim}} = 1500$  N and  $z_{\text{switch}} = 0.02$  m. ( $D = 14.9$ ,  $T_{\text{act}} = 0.04$  s,  $T_{\text{pred}} = 0$ ,  $f_{c\text{lim}}$ ) (a) control input  $f_c$ ; (b) tire deformation  $z_2 - z_0$ ; (c) actuator force  $f_{\text{act}}$ ; (d) actuator force  $f_{\text{act}}$  for  $5.4 \leq t \leq 6.8$  s.



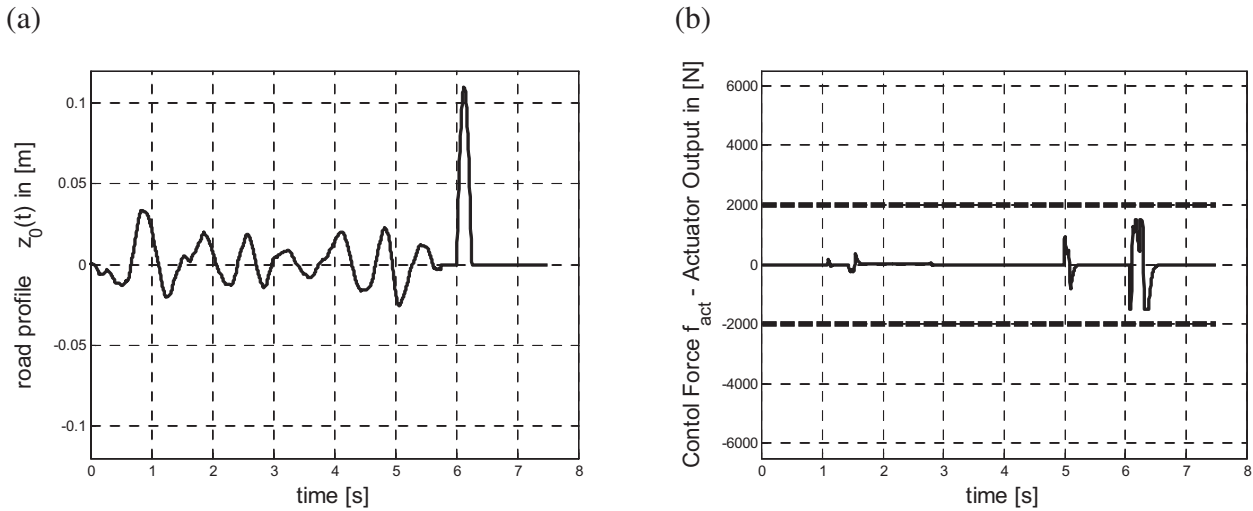


Fig. 11. Actuator effort in case the vehicle travels on a medium roughness road with  $f_{actlim} = 1500$  N and  $z_{switch} = 0.04$  m. ( $T_{act} = 0.04$  s,  $T_{pred} = 0$ ,  $f_{clim} = \infty$ ): (a) road profile  $z_0$ ; (b) actuator force  $f_{act}$ .

Table 6 Performance of the intelligent system for  $f_{actlim} = 1500$  N and optimized  $T_{pred}$  ( $z_{switch} = 0.02$ – $0.04$  m,  $T_{act} = 0.04$  s,  $f_{clim} = \infty$ ).

	$z_{switch}$ [m]		
	0.02	0.03 – $T_{pred} = 1.48$ ms	0.04 – $T_{pred} = 6.61$ ms
Max $ f_{act} $ [N]	1500	1500	1500
Max $ z_R $ [m]	0.0796	0.0796	0.0796
Max $ \ddot{z}_i $ [ $m/s^2$ ]	11.6573	11.8869	12.0207

actuator force is reduced by approximately 60%, while the maximum acceleration is improved by 29%.

Furthermore, the control system is activated only at increased levels of road excitation; see Fig. 10(c) and (d). For a substantial time period the actuator force is zero and therefore the effort is significantly reduced. In order to better demonstrate the resulting advantage the actuator effort for a medium roughness road is plotted in Fig. 11.

In Table 6 the influence of parameter  $T_{pred}$  is shown. Prediction time  $T_{pred}$  is less important for lower threshold  $z_{switch}$  values. The largest improvement is achieved for  $z_{switch} = 0.04$  (if  $z_{switch}$  is varied between 0.02 and 0.04 m) where the maximum acceleration reduces from 13.0288 to 12.0207  $m/s^2$ .

5. Hybrid genetic optimisation

Taking into consideration the number of design parameters, see Eq. (14), the number of constraints, see Eqs. 4–6, the computational cost involved in solving a nonlinear system of differential equations and the objective to minimize acceleration, see Eq. (13), using the smallest actuator it is not efficient to just explore the complete solution space.

In this paper the design problem is formulated as an evolutionary optimisation problem and solved using genetic algorithm. The genetic algorithm is a method for solving both constrained and unconstrained optimisation problems that is based on natural selection, the process that drives biological evolution. The genetic algorithm repeatedly modifies a population of individual solutions. At each step, the genetic algorithm selects individuals from the current population to be parents and uses them to produce the children for the next generation. Over successive generations, the population “evolves” toward an optimal solution. The genetic

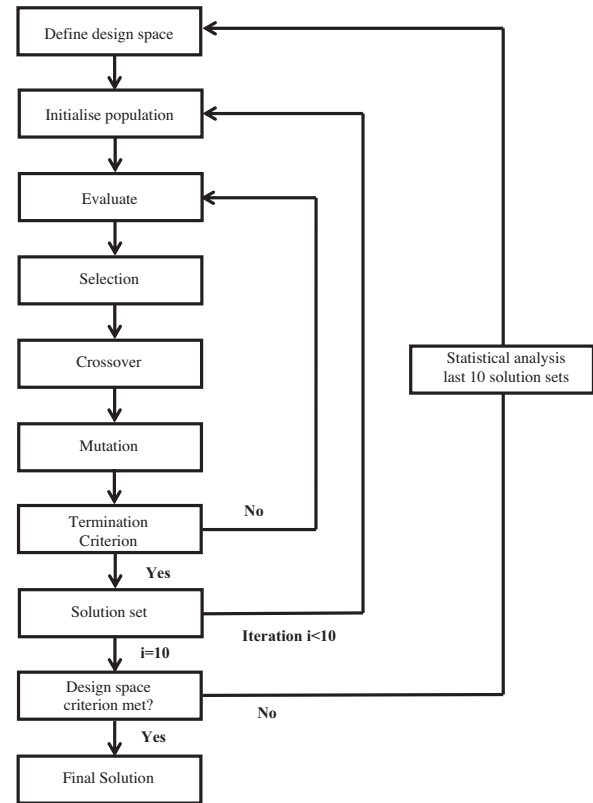


Fig. 12. Schematic of the proposed hybrid genetic algorithm.

algorithm is suitable – in contrast to deterministic optimisation algorithms – for optimizing problems with multiple local minima.

However, in highly nonlinear problems even the genetic algorithm can be trapped in a local minimum. It is highlighted that – for the cases illustrated in the previous section – parameter  $D$  varied in the range  $D \in [7, 21.1]$ . A robust method is needed for improving the probability of success and making it less sensitive to user’s choices. For this purpose a practical procedure based on the combination of statistical analysis and genetic algorithm has been developed. In greater detail:

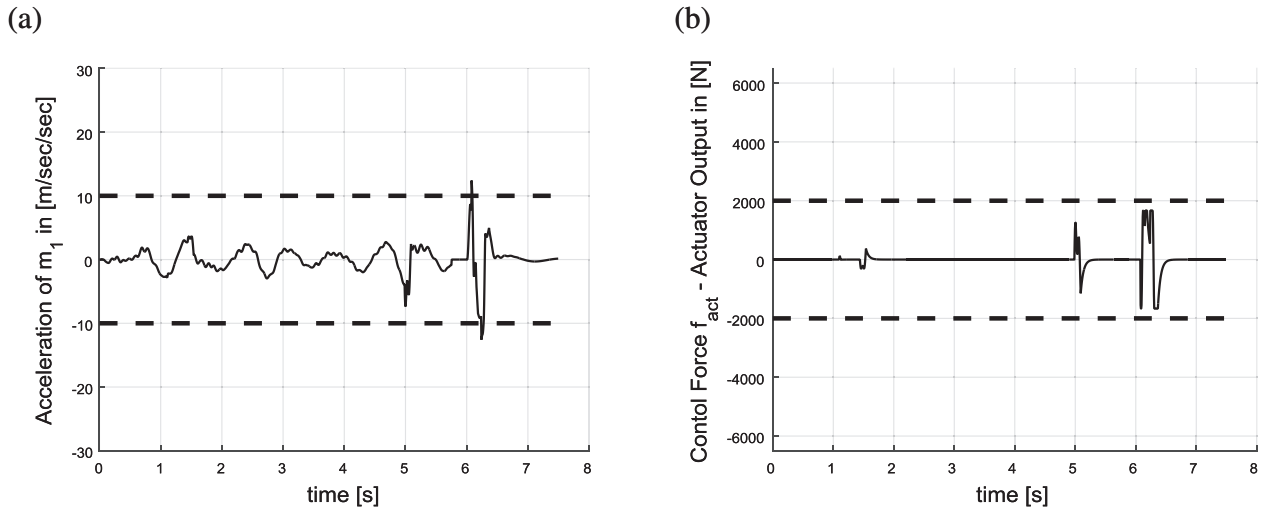


Fig. 13. Actuator effort in case the vehicle travels on a medium roughness road with  $v_{opt} = [14.20.04116680.045]$ .

The genetic algorithm is programmed to generate a population comprised out of fifty members  $v^j = [T_{act}^j, f_{act\ lim}^j, z_{switch}^j, D^j]$ , where  $j = 1 \dots 50$ . The members are selected randomly from a uniform distribution restricted in the design space:  $T_{act}^j \in [0.01, 0.2]$ ,  $f_{act\ lim}^j \in [500, 5000]$ ,  $z_{switch}^j \in [0, 0.08]$  and  $D^j \in [0, 50]$ . The objective function, see Eq. (13), for each member is calculated. Each individual is assigned a score depending on the member's rank and not the objective function value itself. 80% of the new generation is created by crossover and only 5% from the old generation progresses to the new one. A stochastic uniform algorithm is used for selecting the parents and the part of the chromosome that will be used in the crossover operation. The probability for selecting a member as a parent is directly related to its rank. The rest members are created by mutation. The genetic algorithm terminates after 300 generations unless it stalls. It is stalled if for over 200 generations the objective function has not changed significantly. In practice it was found that no more than 100 generations were usually necessary. The solution obtained is an optimized design parameter vector  $v_{opt} = [T_{act-opt}, f_{act\ lim-opt}, z_{switch-opt}, D_{opt}]$ . The solution each time the optimisation problem was solved – even though the settings were exactly the same – was different. In many cases the differences were considerable.

Therefore, in the proposed method the genetic algorithm is employed repeatedly,  $i = 1:10$  and a set of optimized vectors  $v_{opt-i}$  is collected. The statistical parameters (mean value  $\mu$  and standard deviation  $\sigma$ ) of the optimized design parameters are calculated:  $T_{act-opt-\mu}, T_{act-opt-\sigma}, f_{actlim-opt-\mu}, f_{actlim-opt-\sigma}, z_{switch-opt-\mu}, z_{switch-opt-\sigma}$  and  $D_{opt-\mu}, D_{opt-\sigma}$  and used to define the design space in the next optimisation round:  $T_{act}^j \in [T_{act-opt-\mu} - T_{act-opt-\sigma}, T_{act-opt-\mu} + T_{act-opt-\sigma}]$ ,  $f_{actlim}^j \in [f_{actlim-opt-\mu} - f_{actlim-opt-\sigma}, f_{actlim-opt-\mu} + f_{actlim-opt-\sigma}]$ ,  $z_{switch}^j \in [z_{switch-opt-\mu} - z_{switch-opt-\sigma}, z_{switch-opt-\mu} + z_{switch-opt-\sigma}]$  and  $D^j \in [D_{opt-\mu} - D_{opt-\sigma}, D_{opt-\mu} + D_{opt-\sigma}]$ . The loop continues until parameter  $D$  variation becomes less than a predefined threshold. A schematic of the algorithm is shown in Fig. 12.

The proposed method progressively shrinks the design space based on a posterior estimate of the design parameters interval. Practically, the interval reduces first for the parameters that vary less than others and subsequently for the rest. For this problem the design space at the end of the first optimisation round reduced to:  $T_{act}^j \in [0.0452 - 0.0046, 0.0452 + 0.0046]$ ,  $f_{act\ lim}^j \in [2395 - 740.16, 2395 + 740.16]$ ,  $z_{switch}^j \in [0.0461 - 0.0032, 0.0461 + 0.0032]$  and  $D^j \in [18 - 9.46, 18 + 9.46]$  and at the end of the second round the

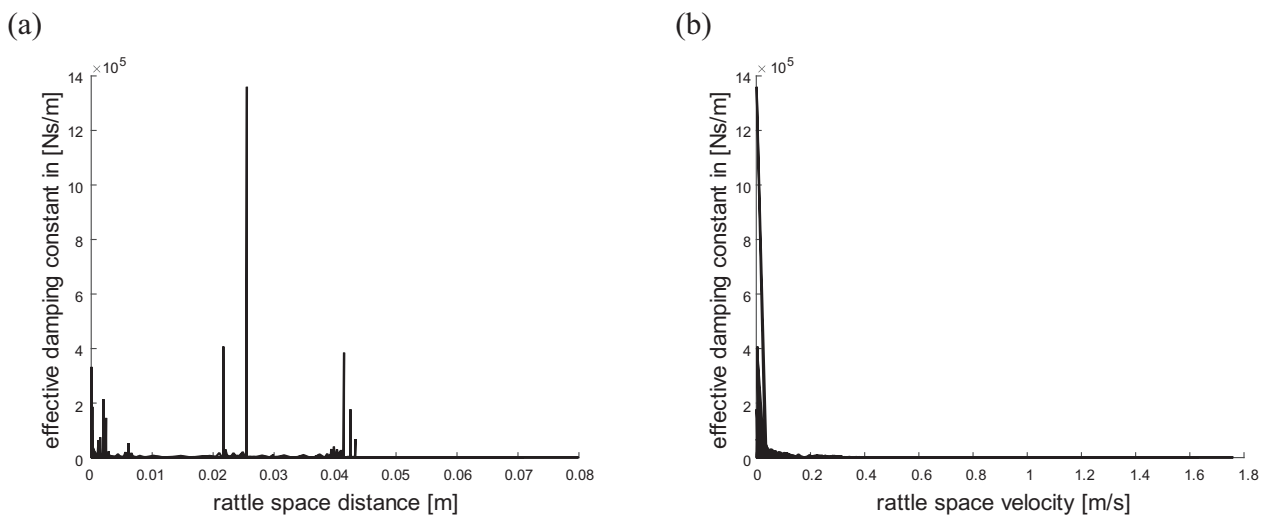


Fig. 14. Optimised effective damping constant  $c_{eff}$  versus: (a) rattles space distance  $z_R$ ; (b) rattles space velocity  $\dot{z}_R$ .

optimized solution was found (parameter  $D$  varied less than 2 units). The optimized design parameter vector was:  $v_{opt} = [14.20.04616680.045]$  and the maximum attained acceleration  $12.56 \text{ m/s}^2$ . In Fig. 13 the sprung mass acceleration and the actuator output are plotted for a vehicle driving on a medium roughness road (like the one shown in Fig. 11).

In Fig. 14 the effective damping constant, which is defined as  $c_{eff} = \frac{c_1 \cdot (\dot{z}_1 - \dot{z}_2) + f_{act}}{z_1 - z_2}$ , versus the rattle space distance and rattle space velocity are plotted.

The figures show that the intelligent system has a high effective damping coefficient for low rattle space velocities and a low one for higher rattle space velocities (see Fig. 14(b)). Furthermore, from Fig. 14(a) it is deduced that the effective damping constant increases in the vicinity of  $z_{switch} = 0.046 \text{ m}$  but also in some cases for lower rattle space distances.

## 6. Conclusions – future research directions

According to the conducted literature survey it is problematic to design vehicle suspension systems that provide superior comfort and handling performance for all road conditions. There is empirical evidence that a large number of vehicles are getting damaged because of road irregularities. There is a trade off balance between conflicting requirements such as vibration reduction, suspension travel, actuator effort, road holding capability, noise and fatigue requirements. Even in case a vehicle is designed to adapt its suspension settings for different road types this is not adequate for discrete and short road excitations such as a pothole.

In this paper, an intelligent road adaptive suspension system is presented for the first time. The backbone of the intelligent system is an experts' based algorithm, which is parameter dependent. The algorithm continuously monitors the road excitation in relation to the suspension travel. The system switches between two modes of operation; a passive and an active one. The active part tries to resemble indirectly Pontryagin's principle. A critical analysis of the design parameters on the system performance is given. The design problem is formulated as an evolutionary optimisation problem with the objective to overcome the trade-off barrier and to minimize the root mean square sprung mass acceleration value using the minimum actuator size. It is shown that the design problem possesses numerous local minima and that even a genetic algorithm gets trapped. A hybrid algorithm that combines statistical analysis and genetic algorithm has been developed and presented in detail. It is shown that the algorithm is more robust in finding the global optimum and makes possible the automation of the design process.

The intelligent suspension system improves significantly the vehicle's performance compared to the passive suspension system (basis), to a conventional semi-active one as well as others found in the literature. The proposed concept succeeds in overcoming the trade-off barrier and more specific it: (a) reduces by more than 50% the maximum acceleration level compared to the semi-active one (b) does not degrade the rattle space and road holding performance (c) minimizes the overall effort of the

controller; the controller becomes active only at high road disturbances and (d) minimizes the size of the required actuator.

Future research activities include the extension of the proposed methodology for optimizing the vehicle's pitch and roll behavior as well as to investigate the performance of the method with an optimized nonlinear passive suspension system.

## References

- Brezas, P., Smith, M., & Hout, W. (2015). A clipped-optimal control algorithm for semi-active vehicle suspensions: Theory and experimental evaluation. *Automatica*, 53, 188–194.
- Brown, R., Pusey, J., Murugan, M., & Le, D. (2013). Generalized predictive control algorithm of a simplified ground vehicle suspension system. *JVC/Journal of Vibration and Control*, 19(16), 2372–2386.
- Gohrle, C., Schindler, A., Wagner, A., & Sawodny, O. (2014). Design and vehicle implementation of preview active suspension controllers. *IEEE Transactions on Control Systems Technology*, 22, 1135–1142.
- Huang, C.-J., Lin, J.-S., & Chen, C.-C. (2010). Road-adaptive algorithm design of half-car active suspension system. *Expert Systems with Applications*, 37(6), 4392–4402.
- Isermann, R. (2003). *Mechatronic systems: Fundamentals*. New York: Springer (Chapter 12).
- Kanarachos, S. A. (2012). Intelligent semi-active vehicle suspension systems using neural networks. *International Journal of Vehicle Systems Modelling and Testing*, 7, 135–158.
- Kanarachos, S. A., Koulocheris, D. V., & Spentzas, K. N. (2005). Synthesis of nonlinear dynamic systems using parameter optimization methods – A case study. *WSEAS Transactions on Computers*, 4(1), 58–63.
- Koch, G., Fritsch, O., & Lohmann, B. (2010). Potential of low bandwidth active suspension control with continuously variable damper. *Control Engineering Practice*, 18(11), 1251–1262.
- Mahmoodabadi, M. J., Adljooy Safaie, A., Bagheri, A., & Nariman-Zadeh, N. (2013). A novel combination of particle swarm optimization and genetic algorithm for Pareto optimal design of a five-degree of freedom vehicle vibration model. *Applied Soft Computing Journal*, 13, 2577–2591.
- Naidu, D. S. (2002). *Optimal control systems*. New York: CRC Press (Chapter 7).
- Nguyen, Q.-H., & Choi, S.-B. (2009). Optimal design of a vehicle magnetorheological damper considering the damping force and dynamic range. *Smart Materials and Structures*, 18.
- Poussot-Vassal, C., Sename, O., Dugard, L., Gáspár, P., Szabó, Z., & Bokor, J. (2008). A new semi-active suspension control strategy through LPV technique. *Control Engineering Practice*, 16, 1519–1534.
- Poussot-Vassal, C., Spelta, C., Sename, O., Savaresi, S. M., & Dugard, L. (2012). Survey and performance evaluation on some automotive semi-active suspension control methods: A comparative study on a single-corner model. *Annual Reviews in Control*, 36, 148–160.
- Savaresi, S., Poussot-Vassal, C., Spelta, C., Sename, O., & Dugard, L. (2010). *Semi-active suspension control design for vehicles*. Butterworth-Heinemann (Chapter 3).
- Soleymani, M., Montazeri-Gh, M., & Amiryan, R. (2012). Adaptive fuzzy controller for vehicle active suspension system based on traffic conditions. *Scientia Iranica*, 19, 443–453.
- Song, C., Zhao, Y., Wang, L., & Niu, L. (2014). Multi-objective optimisation design of passive suspension parameters based on competition-cooperation game model. *Australian Journal of Mechanical Engineering*, 12, 13–24.
- Tung, S.-L., Juang, Y.-T., Lee, W.-H., Shieh, W.-Y., & Wu, W.-Y. (2011). Optimization of the exponential stabilization problem in active suspension system using PSO. *Expert Systems with Applications*, 38(11), 14044–14051.
- Tusset, A. M., Rafikov, M., & Balthazar, J. M. (2009). An intelligent controller design for magnetorheological damper based on a quarter-car model. *Journal of Vibration and Control*, 15, 1907–1920.
- Wang, W., Song, Y., Xue, Y., Jin, H., Hou, J., & Zhao, M. (2015). An optimal vibration control strategy for a vehicle's active suspension based on improved cultural algorithm. *Applied Soft Computing Journal*, 28, 167–174.
- Yim, S.-S., Seok, J.-H., & Lee, J.-J. (2012). State estimation of the nonlinear suspension system based on nonlinear Kalman filter. In International conference on control, automation and systems (pp. 720–725).